Parameter Estimation Method to Improve the Accuracy of Photovoltaic Electrical Model

Emerson A. Silva, Fabricio Bradaschia, *Member, IEEE*, Marcelo C. Cavalcanti, and Aguinaldo J. Nascimento, Jr.

***Abstract*—This paper proposes an estimation method to identify the electrical model parameters of photovoltaic (PV) modules and makes a comparison with other methods already popular in the technical literature. Based on the full single-diode model, the mathematical description of the *I–V* characteristic of modules is generally represented by a coupled nonlinear equation with five unknown parameters, which is difficult to solve by an analytical approach. The aim of the proposed method is to find the five unknown parameters that guarantee the minimum absolute error between the *P–V* curves generated by the electrical model and the *P–V* curves provided by the manufacturers' datasheets for different external conditions such as temperature and irradiance. The first advantage of the proposed method is that the parameters are estimated using the *P–V* curves instead of *I–V* curves, since most of the applications that use the electrical model want to accurately estimate the extracted power. The second advantage is that the value ranges of each unknown parameter respect their physical meaning. In order to prove the effectiveness of the proposition, a comparison among methods is carried out using both types of *P–V* and *I–V* curves: those obtained by manufacturers' datasheets and those extracted experimentally in the laboratory.**

***Index Terms*—Parameter estimation, photovoltaic (PV) cells, PV effects, PV systems.**

I. Introduction

IN most photovoltaic (PV) systems, it is very important to obtain the electrical model parameters of the PV modules connected to the power converter. For example, in order to know the best arrangement of PV array, the adequate design of the power converter and its controller to achieve a desirable dynamic behavior, the best maximum power point (MPP) tracking technique, and the correct estimation of the extracted power based on a real profile of the environmental conditions of a specific place, a series of simulations should be carried out in a specific platform using the PV module electrical model [1], [2]. Therefore, this electrical model must be reliable and accurate in order to predict the energy production from the PV module under different temperature and irradiance conditions. Different kinds of inaccuracy could lead to a wrong decision-making, to an oversize or undersize of the converter, to an instability in the controller or even to an incorrect payback estimation of the investment [3]–[6].

Manuscript received April 27, 2015; revised September 2, 2015; accepted September 11, 2015.

The authors are with the Department of Electrical Engineering, Federal University of Pernambuco, Recife 50670-901, Brazil (e-mail: emerson.silva90@gmail.com; fabricio.bradaschia@ufpe.br; marcelo.cavalcanti@ufpe.br; aguinaldojunior10@hotmail.com).

Color versions of one or more of the figures in this paper are available online at http://ieeexplore.ieee.org.

Digital Object Identifier 10.1109/JPHOTOV.2015.2483369

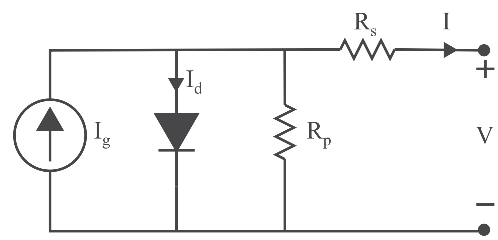

Fig. 1. Equivalent electrical representation of a PV cell.

In practice, a PV module presents nonlinear *I–V* characteristic curves that depend mainly on the cell irradiance and temperature. Based on the physical interpretation of a PV cell and its arrangements to form a PV module, two equivalent electrical models can be built: the single-diode (see Fig. 1) and the double-diode models. The single-diode model [7] consists of four adjustable components: a photogenerated current source, a parallel diode (which presents two adjustable parameters), and a series and a parallel resistance. This model is the most widely used in the technical literature, since it offers a reasonable relationship between simplicity and accuracy [8]. Another advantage of the single-diode model is the possibility to estimate its five unknown parameters based only on information provided by the manufacturers datasheet tables [3], [9], [10].

The *I–V* characteristic curves of the single-diode electrical model are represented by a nonlinear transcendental equation in which the five unknown parameters are mutually coupled. For this reason, it is difficult to determine those parameters using simple analytical methods. One approach to solve this issue is to consider an ideal electrical model for the PV module, i.e., without the series and parallel resistances, as proposed in [11]. Other researchers use constant parameters in their models [12], disregarding the fact that some parameters vary with the temperature or irradiance. In [7], a model was developed through coupled multiphysical processes of PV energy conversion. Due to their simplicity, those methods generate inaccurate models. Other approach is to use optimization and numerical methods or artificial intelligence algorithms to find the parameters that minimize the error between the *I–V* curves generated by the electrical model and the curves experimentally extracted from the PV module [13], [14]. Other methods use a symbolic analysis of the equations that allow one to calculate the values of the series and parallel resistances appearing in the single-diode model of a PV module. The main result is the explicit expressions giving the values of all the five parameters [15]–[17].

Independently of the approach, the methods present three major drawbacks: 1) It requires experimental *I–V* curves, which may not be available to the user; 2) different set of parameters are found for each experimental *I–V* curve obtained, i.e., the estimated parameters lack of physical meaning, since some parameters that should be constant vary with the temperature and irradiance and other parameters that should present a monotonically increasing or decreasing pattern with the temperature or irradiance vary randomly; 3) in those methods, it is the error between *I–V* curves that is minimized, although, in most PV systems, it is desirable to obtain accurate *P–V* curves, mainly near the MPP.

The first drawback is usually solved by using the information provided by the manufacturer datasheets [3], [9], [10], [18], [19]. Although it is possible that the estimated parameters do not match exactly with the physical parameters of the modules, the *I–V* curves generated by the electrical model are usually very close to the experimental curves [8], [12], [20].

Due to these drawbacks, this paper proposes an accurate parameter estimation method for the single-diode electrical model of PV modules. The proposed method presents the following advantages: 1) It estimates the parameters based on selected criteria, *P–V* or *I–V* curves provided by the manufacturer datasheets (does not depend on experimental curves); 2) some restrictions are imposed on each parameter of the model to preserve their physical meaning; 3) the stop criterion of the method is based on the minimization of the error between *P–V* curves or *I–V* curves. In order to prove the effectiveness of the proposed method, a comparison with some popular methods in the literature is carried out using both types of *P–V* curves: those obtained by manufacturers' datasheets and those extracted experimentally in a laboratory.

II. Definition of the Error Metrics

The behavior of a PV cell can be described by an equivalent electrical model (see Fig. 1). The output current of the single-diode model is a function of the output voltage, and it can be described as

$$I = I_g - I_{\text{sat}} \left[e^{\left(\frac{V+IR_s}{V_t}\right)} - 1 \right] - \frac{V + IR_s}{R_p} \tag{1}$$

$$V_t = \frac{N_s AkT}{q} \tag{2}$$

where V and I are the module output voltage and current, I_g is the photogenerated current, I_{sat} is the reverse saturation current of the diode, V_t is the thermal voltage, q is the electron charge, A is the ideality factor of the diode, k is the Boltzmann constant, T is the module temperature, N_s is the number of series connected cells forming the PV module, and R_s and R_p are the series and the parallel resistances, respectively.

The PV module manufacturers do not directly provide the five parameters of the single-diode model. Instead, basically, all datasheets provide the following information for the standard test conditions (STC): open-circuit voltage (V_{oc}), short-circuit current (I_{sc}), MPP voltage (V_{mp}), MPP current (I_{mp}), temperature coefficient for V_{oc} (k_v), temperature coefficient for I_{sc} (k_i), and maximum power (P_{mp}). An analysis of the electrical model in three operation points of the *I–V* curve (I_{sc}, V_{oc}, and P_{mp}) allows relating the unknown parameters of the electrical model to the datasheet information.

The procedure adopted for all parameter estimation methods is this: First, the five unknown parameters are estimated based on the *I–V* or *P–V* curve at the STC; second, the electrical model with the five estimated parameters is simulated not only at the STC but at other conditions provided by the manufacturer datasheets as well; third, a metric is chosen and calculated for each *I–V* or *P–V* curve provided by the manufacturer datasheets. The proposed metric uses the *P–V* curves instead of *I–V* curves, since most of the applications that use the electrical model wants to estimate accurately the extracted power.

The absolute error in power for a specific voltage point is calculated by

$$\text{error}_a = |P_{\text{curve}} - P_{\text{model}}| \tag{3}$$

where P_{curve} is the product of V_{curve} and I_{curve} obtained by the datasheet curve, and P_{model} is the product of V_{model} and I_{model} obtained by the simulation of the electrical model with the parameters estimated by a specific method.

The mean absolute error in power (MAEP) is calculated by

$$\text{MAEP} = \frac{\sum \text{error}_a}{N_{\text{curve}}} \tag{4}$$

where error_a is calculated for all voltage points going from zero to the open-circuit condition and N_{curve} is the number of voltage points extracted from the datasheet *I–V* curve of the PV module.

Similarly to error_a and MAEP, the percentage error (error_p) and the mean percentage error in power (MPEP) can be defined as

$$\text{error}_p = \frac{|P_{\text{curve}} - P_{\text{model}}|}{P_{\text{curve}}} 100\% \tag{5}$$

$$\text{MPEP} = \frac{\sum \text{error}_p}{N_{\text{curve}}}. \tag{6}$$

It now remains to define which of the two error metrics is the most suitable for calculating the errors between the datasheet curves and the ones generated by the electrical model. In the areas where the PV power is low, any difference between the datasheet curve and the model curve is amplified in error_p. Moreover, if the same difference between the datasheet curve and the model curve occurs in the MPP, it will be attenuated in error_p. Therefore, the metric MPEP give more importance to differences that occurs in areas where the PV power is low, as can be seen in Fig. 2. A different effect occurs with the metric MAEP: Since it is based on the absolute error, the same difference in two different points of the *P–V* curve will have the same importance. Nevertheless, due to the high absolute power values near the MPP, it is more likely that the differences between curves are greater in this region. The opposite effect occurs in areas where the PV power is low. Therefore, the metric MAEP gives more importance to differences near the MPP, as can be seen in Fig. 2. This is the reason for choosing the metric MAEP as a figure of merit for comparing methods. Therefore, the average value of the MAEP is calculated considering all *P–V* curves, in order to make a fair comparison among the methods. It is important to observe that for each *P–V* curve of the datasheet,

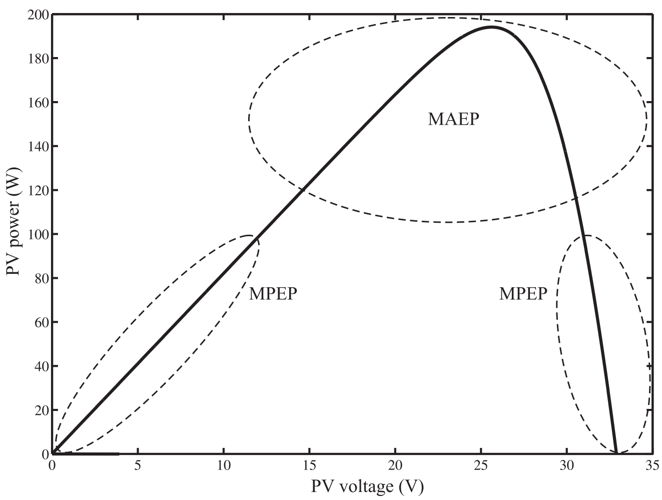

Fig. 2. Regions of MPEP and MAEP.

different values of short-circuit current and open-circuit voltage are obtained, defining different starting and ending points of the electrical model simulation for all estimation methods.

III. Photovoltaic Parameter Estimation Methods

A. *Xiao's Method [12]*

This method relies on the fact that, in a PV module, the derivative of the power regarding the voltage is zero at the MPP. It is possible to find the photogenerated current and the open-circuit voltage as

$$I_g = [I_{\text{sc,STC}} + k_i(T - T_R)]\frac{S}{1000} \tag{7}$$

$$V_{\text{oc}} = V_{\text{oc,STC}} + k_v(T - T_R) \tag{8}$$

where T_R is the reference temperature. Using (1), it is possible to find the diode saturation current and the current in the MPP:

$$I_{\text{sat}} = \frac{I_g - \frac{V_{\text{oc}}}{R_p}}{e^{\frac{V_{\text{oc}}}{V_t}} - 1} \tag{9}$$

$$I_{\text{mp}} = I_g - I_{\text{sat}}\left[e^{\left(\frac{V_{\text{mp}}+I_{\text{mp}}R_s}{V_t}\right)} - 1\right] - \frac{V_{\text{mp}} + I_{\text{mp}}R_s}{R_p}. \tag{10}$$

The influence of the parallel resistance is neglected, allowing (9) and (10) be rewritten as

$$I_{\text{sat}} = \frac{I_g}{e^{\left(\frac{V_{\text{oc}}}{V_t}\right)} - 1} \tag{11}$$

$$I_{\text{mp}} = I_g - I_{\text{sat}}\left[e^{\left(\frac{V_{\text{mp}}+I_{\text{mp}}R_s}{V_t}\right)} - 1\right]. \tag{12}$$

Substituting (11) into (12) yields

$$R_s = \frac{V_t \ln\left[\left(1 - \frac{I_{\text{mp}}}{I_g}\right)e^{\left(\frac{V_{\text{oc}}}{V_t}\right)} + \frac{I_{\text{mp}}}{I_g}\right] - V_{\text{mp}}}{I_{\text{mp}}}. \tag{13}$$

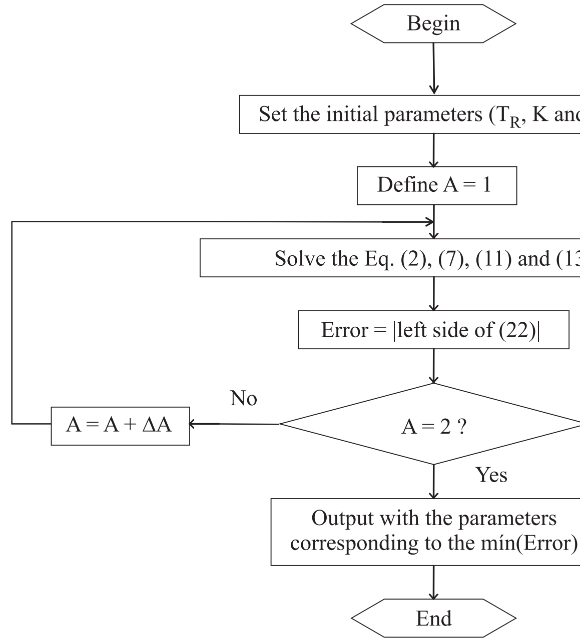

Fig. 3. Xiao method flowchart.

Then, taking the derivative of the power with respect to voltage in the MPP condition:

$$-\frac{\frac{I_{\text{sat}}}{V_t}e^{\left(\frac{V_{\text{mp}}+I_{\text{mp}}R_s}{V_t}\right)}}{1 + \frac{I_{\text{sat}}R_s}{V_t}e^{\left(\frac{V_{\text{mp}}+I_{\text{mp}}R_s}{V_t}\right)}} + \frac{I_{\text{mp}}}{V_{\text{mp}}} = 0. \tag{14}$$

Thus, in Xiao's method, four parameters are completely defined by analytical equations. The fifth parameter, A, is varied from 1 to 2 and, for each value of A, the term on the left side of (14) is calculated. The set (A, R_s, I_{sat} e I_g) that minimizes left side of (14) represents the estimated parameters of the PV module. The flowchart of this method is shown in Fig. 3.

B. *Villalva's Method [8]*

This method intends to adjust R_s and R_p based on the fact that there is only one pair (R_s, R_p), which guarantees that $P_{\text{mp,model}} = P_{\text{mp,curve}} = V_{\text{mp}}I_{\text{mp}}$ at the MPP (V_{mp}, I_{mp}) of the *I–V* curve, i.e., the maximum power based on the simulated electrical model ($P_{\text{mp,model}}$) is equal to the maximum power obtained from the datasheet curve ($P_{\text{mp,curve}}$) at V_{mp}.

First, the authors assume that the ideality factor A can be chosen arbitrarily, assuming a constant value (in [8], A is equal to 1.3), and then, it can be changed to better fit the *I–V* curve, if necessary. Thus, the relationship between R_s and R_p in (1) can be found by making $P_{\text{mp,model}} = P_{\text{mp,curve}}$ and solving the resulting equation for R_p, as follows:

$$R_p = \frac{V_{\text{mp}}(V_{\text{mp}} + R_sI_{\text{mp}})}{V_{\text{mp}}\left[I_g - I_{\text{sat}}\left(e^{\left(\frac{V_{\text{mp}}+R_sI_{\text{mp}}}{V_t}\right)} - 1\right)\right] - P_{\text{mp,curve}}}. \tag{15}$$

Equation (15) indicates that, for any value of R_s, there will be a single value of R_p that makes the electrical model goes through the point (V_{mp}, I_{mp}) defined in datasheet.

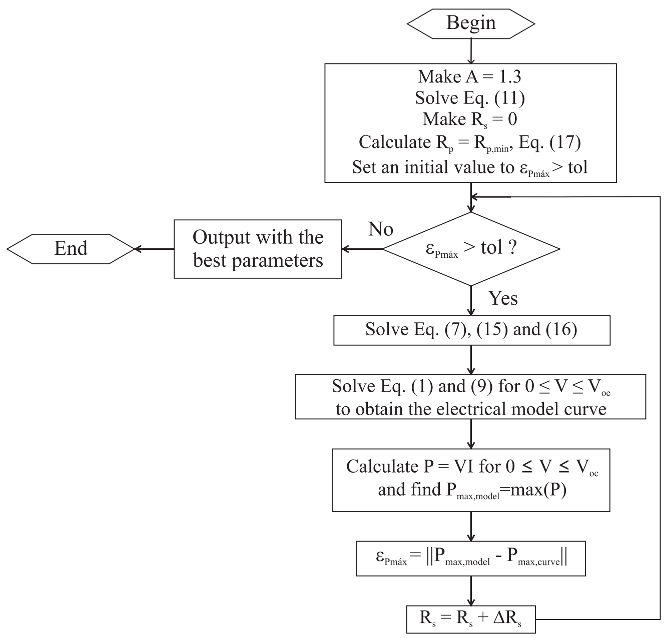

Fig. 4. Villalva method flowchart.

This method also uses an iterative solution with R_s and R_p, which updates the value of I_g each iteration, since it assumes $I_g \neq I_{\text{sc}}$. Thus, neglecting I_{sat}, it is found that

$$I_{g,\text{STC}} = \frac{R_p + R_s}{R_p} I_{\text{sc,STC}}. \tag{16}$$

Finally, initial values for R_s and R_p are still needed before the iterative process start up. The initial value of R_s is zero, while the initial value of R_p is defined by the authors as

$$R_{p,\min} = \frac{V_{\text{mp}}}{I_{\text{sc}} - I_{\text{mp}}} - \frac{V_{\text{oc}} - V_{\text{mp}}}{I_{\text{mp}}} \tag{17}$$

where all the voltage and current values are defined at STC. The flowchart of the Villalva's method can be seen in Fig. 4.

C. Nonlinear Least Square (NLS) Method [21]

This estimation method is based on solving the nonlinear system with five variables (A, R_s, R_p, I_g, I_{sat}) through five objective functions. These objective functions are based on the equations related to the short-circuit, the open-circuit, the MPP conditions of the PV module, and two other equations.

Thus, the five objective functions used in this method can be written as follows:

$$f_1(x) = 0 = I_g - I_{\text{sat}}\left[e^{\frac{I_{\text{sc}} R_s}{V_t}} - 1\right] - \frac{I_{\text{sc}} R_s}{R_p} - I_{\text{sc}} \tag{18}$$

$$f_2(x) = 0 = I_{\text{sat}}\left[e^{\frac{V_{\text{oc}}}{V_t}} - 1\right] + \frac{V_{\text{oc}}}{R_p} - I_g \tag{19}$$

$$f_3(x) = 0 = I_g - I_{\text{sat}}\left[e^{\frac{V_{\text{mp}} + I_{\text{mp}} R_s}{V_t}} - 1\right] - \frac{V_{\text{mp}} + I_{\text{mp}} R_s}{R_p} - I_{\text{mp}} \tag{20}$$

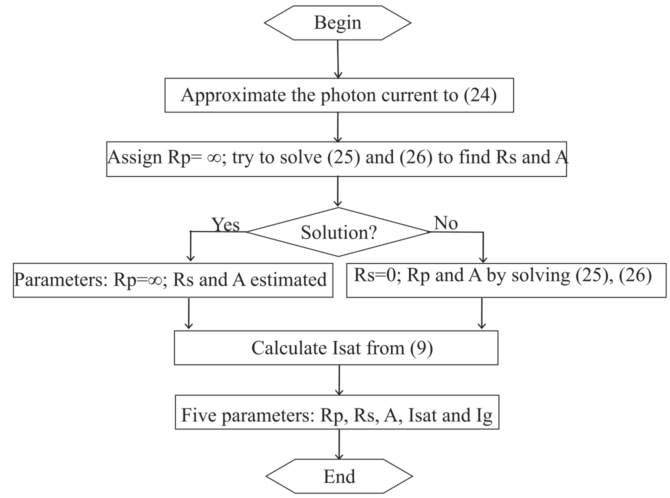

Fig. 5. Mahmoud method flowchart.

$$f_4(x) = 0 = V_{\text{mp}}\left[\frac{\frac{I_{\text{sat}}}{V_t} e^{\left(\frac{V_{\text{mp}} + R_s I_{\text{mp}}}{V_t}\right)} + \frac{1}{R_p}}{1 + \frac{R_s I_{\text{sat}}}{V_t} e^{\left(\frac{V_{\text{mp}} + R_s I_{\text{mp}}}{V_t}\right)} + \frac{R_s}{R_p}}\right] - I_{\text{mp}} \tag{21}$$

$$f_5(x) = 0 = \frac{\frac{I_{\text{sat}}}{V_t} e^{\left(\frac{R_s I_{\text{sc}}}{V_t}\right)} + \frac{1}{R_p}}{1 + \frac{R_s I_{\text{sat}}}{V_t} e^{\left(\frac{R_s I_{\text{sc}}}{V_t}\right)} + \frac{R_s}{R_p}} - \frac{1}{R_p}. \tag{22}$$

The minimization of these five objective functions is obtained by the command *fsolve* in MATLAB, which ensures that

$$x = \left[A, R_s, R_p, I_g, I_{\text{sat}}\right]\Big|_{x_{\min}}^{x_{\max}} \rightarrow \min \left[f_1^2(x) + f_2^2(x) + f_3^2(x) + f_4^2(x) + f_5^2(x)\right] \tag{23}$$

where $x_{\min}$ and $x_{\max}$ represent the lower and upper bounds by which the model parameters are restricted, in order to avoid a parameter to assume values with no physical meaning.

D. Mahmoud's Method [22]

In this method, the authors propose an approach for PV models to improve modeling accuracy and reduce implementation complexity. They develop a method to estimate circuit parameters relying only on the points provided by all commercial modules datasheet in the STC. The five parameters are calculated by using the following equations:

$$I_g = I_{\text{sc}} \tag{24}$$

$$I_{\text{mp}} = I_g - I_{\text{sat}}\left[e^{\frac{(V_{\text{mp}} + I_{\text{mp}} R_s)}{V_t}} - 1\right] - \frac{V_{\text{mp}} + I_{\text{mp}} R_s}{R_p} \tag{25}$$

$$\frac{dP}{dV} = I_{\text{sc}} - I_{\text{sat}}\left[e^{\frac{(V_{\text{mp}} + I_{\text{mp}} R_s)}{V_t}} - 1\right] - \frac{V_{\text{mp}} + I_{\text{mp}} R_s}{R_p} + V_{\text{mp}}\left[-\frac{1}{V_t} I_{\text{sat}} e^{\frac{(V_{\text{mp}} + I_{\text{mp}} R_s)}{V_t}} - \frac{1}{R_p}\right] = 0. \tag{26}$$

The flowchart of Mahmoud's method is seen in Fig. 5.

This article has been accepted for inclusion in a future issue of this journal. Content is final as presented, with the exception of pagination.

E. Accarino's Method (Explicit Equations)[15]

In this method, a symbolic analysis is used to calculate the values of the series and parallel resistances. It allows one to identify the parameters values in the STC and requires a solution of a nonlinear system of equations. The problem is afforded by using symbolic calculations and explicit expressions give the values of all the five parameters. I_g is calculated from (24), and the other parameters are calculated as follows:

$$
\begin{aligned}
A &= \frac{k_v - \frac{V_{oc}}{T}}{\frac{N_s k T}{q} \cdot \left(\frac{k_i}{I_g} - \frac{3}{T} - \frac{E_{\text{gap}}}{kT^2}\right)} \\
I_{\text{sat}} &= I_g \cdot e^{-\frac{V_{oc}}{V_t}} \\
R_s &= \frac{xV_t - V_{\text{mp}}}{I_{\text{mp}}} \\
R_p &= \frac{xV_t}{I_g - I_{\text{mp}} - I_{\text{sat}} \cdot (e^x - 1)}
\end{aligned} \tag{27}
$$

where E_{gap} is the bandgap of the semiconductor material, and x is given by

$$
x = W\left[\frac{V_{\text{mp}}(2I_{\text{mp}} - I_g)e^{\frac{V_{\text{mp}}(V_{\text{mp}} - 2V_t)}{V_t^2}}}{I_{\text{sat}}V_t}\right] + 2\frac{V_{\text{mp}}}{V_t} - \frac{V_{\text{mp}}^2}{V_t^2} \tag{28}
$$

where W is the Lambert function [15].

F. Proposed Method

After a careful analysis of the methods previously mentioned, it is possible to observe some clear disadvantages. Since Xiao's method neglects the influence of R_p, a PV module that presents considerably low values of R_p cannot be accurately represented by this method. Mahmoud's method has similar problem to Xiao's method since it neglects the influence of R_p or R_s. Villalva's method is accurate near the MPP, since its equation goes through the MPP, but maybe it can be inaccurate at other regions of the *I–V* curve. In addition, during the minimization interactions of the NLS method, it could get stuck in a local minimum that does not represent the most accurate set of parameters of the PV module. In [15], it is stated that Accarino's method can be used as guess solution for a more accurate calculation, indicating that this method is not precise.

The proposed method tries to solve the limitations found in previous methods. In order to avoid the mentioned problems, a complete scan of all possible values of A (from 1 to 2 with a step of 0.01) and R_s (from 0 to 2 Ω with a step of 1 mΩ) is made. The other three parameters are defined as follows: I_g is given by (7), I_{sat} is obtained from (9), and R_p is isolated in (10), yielding

$$
R_p = \frac{V_{oc}\left[\frac{e^{\left(\frac{V_{\text{mp}} + I_{\text{mp}}R_s}{V_t}\right)} - 1}{e^{\left(\frac{V_{oc}}{V_t}\right)} - 1}\right] - V_{\text{mp}} - I_{\text{mp}}R_s}{I_{\text{mp}} + I_g\left\{\left[\frac{e^{\left(\frac{V_{\text{mp}} + I_{\text{mp}}R_s}{V_t}\right)} - 1}{e^{\left(\frac{V_{oc}}{V_t}\right)} - 1}\right] - 1\right\}}. \tag{29}
$$

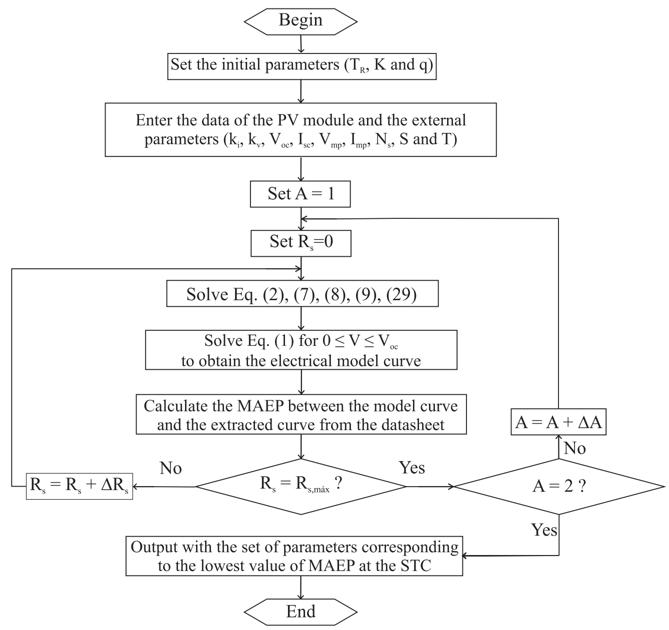

Fig. 6. Proposed method 1 flowchart.

Thereafter, the best set of parameters is chosen based on the lowest value of MAEP calculated between the curve generated by the electrical model and the curve extracted from the datasheet (or from the experimental curve) at the STC in a complete scan. This means that the proposed method chooses the set of parameters, which generates the most accurate *P–V* curve when compared with the datasheet (or the experimental curve), i.e., the curve with the lowest MAEP. The flowchart of the proposed method can be seen in Fig. 6.

The proposed method assumes that the parameters R_p and A do not depend on the temperature or irradiance, i.e., are constants. Since the parameters I_g and I_{sat} depend on I_{sc} and V_{oc}, both depend on the temperature and irradiance. The remaining parameter is the series resistance R_s. The series resistance of a PV module represents the ohmic resistances of the connections and contacts, which increase with the temperature, and the internal resistance of the p-n junction of the PV module, which increases as the irradiance decreases [23]. Thus, based on results of datasheet and experiment, the proposed expression that represents these behaviors is given by

$$
R_s = R_{s,\text{STC}}\underbrace{[1 + k_{Rs}(T - T_R)]}_{\text{Variation with } T.}\underbrace{\left(\frac{S}{1000}\right)^{-B}}_{\text{Variation with } S.} \tag{30}
$$

where k_{Rs} is the linear temperature coefficient, and B is the exponential irradiance coefficient of the series resistance. In (30), $R_{s,\text{STC}}$ is the value of the series resistance estimated by the proposed method at the STC. Therefore, the parameters to be determined are k_{Rs} and B.

For obtaining the k_{Rs} coefficient, its value was varied from 0 to 0.5 $\%/C$ with a step of 0.1 $\%/C$. For each k_{Rs}, the *P–V* curves are simulated for all temperature conditions available on the datasheet (maintaining the irradiance constant). The next step is to compare all curves with those available on the datasheet and

This article has been accepted for inclusion in a future issue of this journal. Content is final as presented, with the exception of pagination.

to calculate the average value of MAEP. Then, the coefficient k_{Rs} is chosen based on the lowest average value of MAEP for these comparisons.

For obtaining the B coefficient, a simplified version of the procedure shown in Fig. 6 is carried out. First, the best values of R_s are obtained through complete scans at different irradiance and same temperature, maintaining the parameters A and R_p constant and equal to the values found in the first estimation. After obtaining the best value of R_s for each irradiance value available on the datasheet, a curve-fitting algorithm is carried out in order to find a suitable value for the coefficient B.

In this paper, the proposal is using MAEP as error metric, but other performance index defined in [22] is also presented here. The root-mean-square deviation (RMSD) of the PV current will also be used to evaluate the modeling accuracy. The RMSD and normalized RMSD (NRMSD) of the model-generated PV current array $\widetilde{I}$ with respect to the measured values I can be expressed as follows:

$$\mathrm{RMSD} = \sqrt{\frac{\sum_{j=1}^{N_{\text{curve}}} (\widetilde{I}_j - I_j)^2}{N_{\text{curve}}}}$$

$$\mathrm{NRMSD} = \frac{\mathrm{RMSD}}{I_{\text{sc}}} \cdot 100\%. \tag{31}$$

Based on this performance index, a second proposal can be made in this paper: The best set of parameters is chosen based on the lowest value of RMSD calculated between the curve generated by the electrical model and the curve extracted from the datasheet at the STC in a complete scan. This means that the proposed method chooses the set of parameters, which generates the most accurate *I–V* curve when compared with the datasheet, i.e., the curve with the lowest RMSD. The flowchart of this second proposed approach is similar to that in Fig. 6, only changing from MAEP to RMSD.

IV. Comparison Results

In order to make a fair comparison among the presented methods, datasheet and experimental curves of two different Kyocera PV modules are considered. The datasheet curves were extracted using a curve extractor algorithm developed in MATLAB platform. The experimental curves were obtained using an experimental setup that included accurate voltage and current probes (to measure the output voltage and current), a pyranometer (to measure the irradiance), and a temperature sensor. With all curves available, each estimation method is executed, the best set of parameters is obtained, and the electrical model is simulated for all curves in order to obtain the average value of MAEP and NRMSD.

A. Photovoltaic Module KC200GT—Datasheet Curves

Table I shows the comparison results obtained for the module KC200GT, a multicrystal PV module from Kyocera. All parameters are defined at the STC. Four performance indexes are shown in Table I: MAEP and NRMSD (both at STC), and $\mathrm{MAEP_{av}}$ and $\mathrm{NRMSD_{av}}$ (average MAEP and NRMSD considering all tested temperature and irradiance conditions). In proposal 1, $k_{Rs} = 0.1$ and $B = 0.77$ are chosen, while in proposal 2, $k_{Rs} = 0.2$ and $B = 0.78$ are chosen for using in (30).

TABLE I
Comparison Among Estimation Methods for Module KC200GT

Methods*	**A**	**B**	**C**	**D**	**E**	**F**	**G**
Factor **A**	1.346	1.300	1.241	1.412	1.079	1.000	1.000
$\mathbf{R_s\,(m\Omega)}$	163.4	138.7	198.4	131.4	236.8	271.0	269.0
$\mathbf{R_p\,(\Omega)}$	∞	466.0	599.9	∞	204.0	171.2	166.7
$\mathbf{I_g\,(A)}$	8.193	8.193	8.193	8.193	8.193	8.193	8.193
$\mathbf{I_{sat}\,(nA)}$	161.1	85.2	35.8	367.0	2.0	0.3	0.3
$\mathbf{MAEP\,(W)}$	1.98	2.54	1.48	2.30	0.98	**0.48**	0.49
$\mathbf{MAEP_{av}}$ (W)	1.85	2.13	1.59	1.97	1.48	**0.72**	0.73
$\mathbf{NRMSD}$(%)	1.41	1.85	1.06	1.64	0.67	**0.36**	**0.36**
$\mathbf{NRMSD_{av}}$ (%)	2.23	2.61	2.06	2.30	2.24	**1.34**	1.37

*Methods: A—Xiao, B—Villalva, C—NLS, D—Mahmoud, E—Accarino, F—Proposal 1 (MAEP), G—Proposal 2 (RMSD(I)).

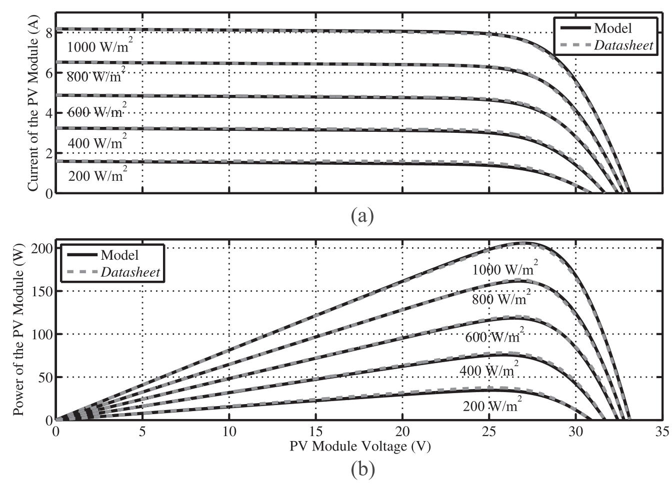

Fig. 7. Proposed method 1: Comparison between the model and the datasheet curves for the module KC200GT at different irradiances for 25 °C.

As can be seen, the proposed method 1 (see F in Table I) obtained the best results of MAEP at the STC and the lowest $\mathrm{MAEP_{av}}$ and $\mathrm{NRMSD_{av}}$ for seven curves at different temperature and irradiance conditions (see Fig. 7 for 25 °C and Fig. 8 for 1000 W/m^2). The proposed method 2 (see G in Table I) obtained the best results for the NRMSD at the STC, as expected, since it was developed to minimize the error in this situation. Then, it can be concluded that the proposed methods obtained the most accurate electrical model for the PV module KC200GT.

B. Photovoltaic Module KS20T—Experimental Curves

Table II shows the comparison results obtained for the module KS20T, a multicrystal PV module from Kyocera. All parameters are defined at the STC. Four performance index are shown in Table II: MAEP and NRMSD (both at STC), and $\mathrm{MAEP_{av}}$ and $\mathrm{NRMSD_{av}}$ (average MAEP and NRMSD considering all tested temperature and irradiance conditions). The Accarino's method could not be compared in the module KS20T because it does not present k_v and k_i values in datasheet.

As can be seen, the proposed methods 1 and 2 once again obtained the best results of the four performance index for five

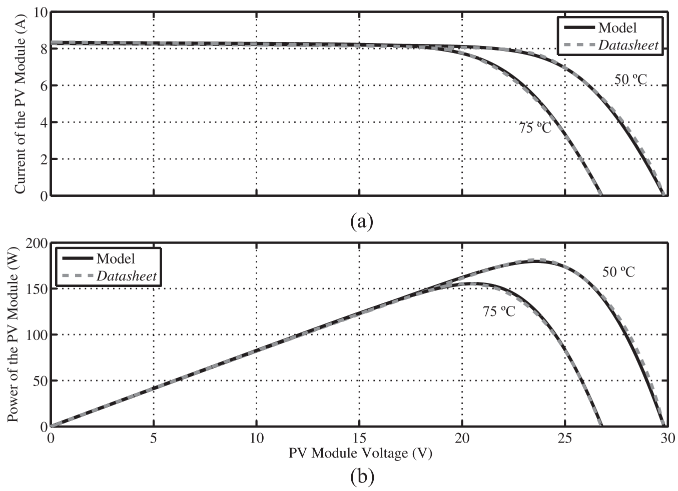

Fig. 8. Proposed method 1: Comparison between the model and the datasheet curves for the module KC200GT at different temperatures for $1000\ \mathrm{W/m^2}$.

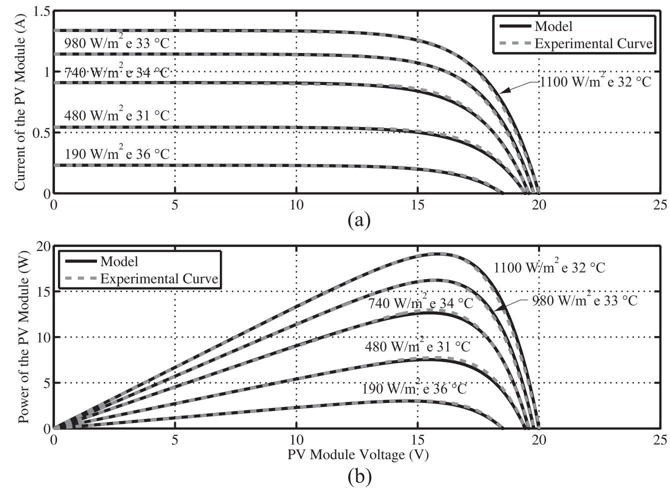

Fig. 9. Proposed method 1: comparison between the estimated electrical model and the experimental curves for the module KS20T at different temperatures and irradiances.

TABLE II
COMPARISON AMONG ESTIMATION METHODS FOR MODULE KS20T

Methods*	**A**	**B**	**C**	**D**	**E**	**F**	**G**
$\mathbf{A}$	1.755	1.400	1.468	1.821	-	1.600	1.600
$\mathbf{R_s\,(m\Omega)}$	177.9	587.2	593.0	132.8	-	437.0	441.0
$\mathbf{R_p\,(\Omega)}$	∞	590.8	922.1	∞	-	2667.7	2818.0
$\mathbf{I_g\,(A)}$	1.143	1.143	1.143	1.143	-	1.143	1.143
$\mathbf{I_{sat}\,(\mu A)}$	7.83	0.37	0.53	9.01	-	2.46	2.46
$\mathbf{MAEP(W)}$	0.07	0.06	0.05	0.08	-	**0.04**	**0.04**
$\mathbf{MAEP_{av}}$ (W)	0.07	0.07	**0.06**	0.07	-	**0.06**	**0.06**
$\mathbf{NRMSD}(\%)$	0.46	0.43	0.31	0.54	-	**0.23**	**0.23**
$\mathbf{NRMSD_{av}}\,(\%)$	0.72	1.22	0.85	0.85	-	0.56	**0.55**

*Methods: A—Xiao, B—Villalva, C—NLS, D—Mahmoud, E—Accarino F—Proposal 1 (MAEP), G—Proposal 2 (RMSD(I)).

curves at different irradiance conditions (see Fig. 9). Then, it can be concluded that the proposed methods obtained the most accurate electrical model for the PV module KS20T.

Observing Tables I and II, the proposed methods present the best results in both metrics when compared with five well-known methods. Most of the parameter estimation methods published in the literature determines the five parameters of the PV model only based on the *I–V* curve in STC. If one uses the same parameters (A, R_s, and R_p, since $I_{\rm sat}$ and I_g change with the temperature and irradiance) in the PV model for other environmental conditions, the *I–V* curve will not follow the expected experimental curve. Thus, in order to obtain accurate results for different environmental conditions, those papers obtain different sets of the five parameters, each set for each experimental curve. Although the results seem good, the physical meaning of the parameters is completely lost, since the parameters change randomly with the temperature and irradiance. For this reason, the proposed method aims the preservation of the physical meaning of the parameters, i.e., A is fixed, R_p is fixed, R_s changes like (30), $I_{\rm sat}$ changes like (9), and I_g changes like (7). Thus, in the proposed method, it is not necessary to run the algorithm for every different experimental curve obtained. The idea is that the PV model would extrapolate new *I–V* curves (with different environmental conditions) based only on the curves used to obtain the five parameters in the proposed method. The two-parameter iteration approach was used to improve the curve fitting in STC. In the proposed method, I_g ensures the short-circuit point, $I_{\rm sat}$ ensures the open-circuit point, and R_p ensures the MPP point. The parameters A and R_s are scanned in order to fit the STC curve and to find the set of parameters that give the lowest value of MAEP or NRMSD.

V. CONCLUSION

This paper has presented some characteristics that are novelty in the literature. A new error metric MAEP was defined. The MAEP holds the proportionality among the errors and gives equal importance to all areas of the *P–V* curve. Two different methods are proposed, based on two different error metrics: MAEP and NRMSD. The proposed methods 1 and 2 scan A and R_s and choose the set of parameters that gives the minimum value of MAEP and NRMSD, respectively, for the STC. A and R_s were chosen as the iteration parameters because of their capability to change the entire *I–V* curve. Using the two-parameter iteration approach, better results are found among all well-known methods shown in the comparison.

REFERENCES

[1] M. Sitbon, J. Leppaaho, T. Suntio, and A. Kuperman, "Dynamics of photovoltaic-generator-interfacing voltage-controlled buck power stage," *IEEE J. Photovoltaics*, vol. 5, no. 2, pp. 633–640, Mar. 2015.

[2] E. Dall'Anese, S. V. Dhople, B. B. Johnson, and G. B. Giannakis, "Optimal dispatch of residential photovoltaic inverters under forecasting uncertainties," *IEEE J. Photovoltaics*, vol. 5, no. 1, pp. 350–359, Jan. 2015.

[3] A. Chatterjee, A. Keyhani, and D. Kapoor, "Identification of photovoltaic source models," *IEEE Trans. Energy Convers.*, vol. 26, no. 3, pp. 883–889, Sep. 2011.

[4] K. Ruhle, M. K. Juhl, M. D. Abbott, and M. Kasemann, "Evaluating crystalline silicon solar cells at low light intensities using intensity-dependent analysis of IV parameters," *IEEE J. Photovoltaics*, vol. 5, no. 3, pp. 926–931, May 2015.

[5] K. J. Sauer, T. Roessler, and C. W. Hansen, "Modeling the irradiance and temperature dependence of photovoltaic modules in PVsyst," *IEEE J. Photovolt.*, vol. 5, no. 1, pp. 152–158, Jan. 2015.

[6] B. Romero *et al.*, "Circuital model validation for S-shaped organic solar cells by means of impedance spectroscopy," *IEEE J. Photovoltaics*, vol. 5, no. 1, pp. 234–237, Jan. 2015.

[7] S. Liu and R. A. Dougal, "Dynamic multiphysics model for solar array," *IEEE Trans. Energy Convers.*, vol. 17, no. 2, pp. 285–294, Jun. 2002.

[8] M. G. Villalva, J. R. Gazoli, and E. F. Ruppert, "Comprehensive approach to modeling and simulation of photovoltaic arrays," *IEEE Trans. Power Electron.*, vol. 24, no. 5, pp. 1198–1208, May 2009.

[9] R. Kadri, J. P. Gaubert, and G. Champenois, "An improved maximum power point tracking for photovoltaic grid-connected inverter based on voltage-oriented control," *IEEE Trans. Ind. Electron.*, vol. 58, no. 1, pp. 66–75, Jan. 2011.

[10] A. Yazdani *et al.*, "Modeling guidelines and a benchmark for power system simulation studies of three-phase single-stage photovoltaic systems," *IEEE Trans. Power Del.*, vol. 26, no. 2, pp. 1247–1264, Apr. 2011.

[11] Y. A. Mahmoud, W. Xiao, and H. H. Zeineldin, "A simple approach to modeling and simulation of photovoltaic modules," *IEEE Trans. Sustain. Energy*, vol. 3, no. 1, pp. 185–186, Jan. 2012.

[12] W. Xiao, W. G. Dunford, and A. Capel, "A novel modeling method for photovoltaic cells," in *Proc. IEEE Power Electron. Spec. Conf.*, 2004, pp. 1950–1956.

[13] J. A. Jervase, H. Bourdoucen, and A. Al-Lawati, "Solar cell parameter extraction using genetic algorithms," *Meas. Sci. Technol.*, vol. 12, no. 11, pp. 1922–1925, 2001.

[14] M. A. D. Blas, J. L. Torres, E. Prieto, and A. Garcia, "Selecting a suitable model for characterizing photovoltaic devices," *Renewable Energy*, vol. 25, no. 3, pp. 371–380, 2002.

[15] J. Accarino, G. Petrone, C. A. Ramos-Paja, and G. Spagnuolo "Symbolic algebra for the calculation of the series and parallel resistances in PV module model," in *Proc. Int. Conf. Clean Electr. Power*, 2013, pp. 62–66.

[16] E. I. Batzelis, I. A. Routsolias, and S. A. Papathanassiou, "An explicit PV string model based on the Lambert W function and simplified MPP expressions for operation under partial shading," *IEEE Trans. Sustain. Energy*, vol. 5, no. 1, pp. 301–312, Jan. 2014.

[17] S. Shongwe and M. Hanif, "Comparative analysis of different single-diode PV modeling methods," *IEEE J. Photovoltaics*, vol. 5, no. 3, pp. 938–946, May 2015.

[18] F. Adamo, F. Attivissimo, A. D. Nisio, and M. Spadavecchia, "Characterization and testing of a tool for photovoltaic panel modeling," *IEEE Trans. Instrum. Meas.*, vol. 60, no. 5, pp. 1613–1622, May 2011.

[19] C. Liu, K. T. Chau, and X. Zhang, "An efficient wind-photovoltaic hybrid generation system using doubly excited permanent-magnet brushless machine," *IEEE Trans. Ind. Electron.*, vol. 57, no. 3, pp. 831–839, Mar. 2010.

[20] W. Xiao, W. G. Dunford, P. R. Palmer, and A. Capel, "Regulation of photovoltaic voltage," *IEEE Trans. Ind. Electron.*, vol. 54, no. 3, pp. 1365–1374, Jun. 2007.

[21] B. K. Nayak, A. Mohapatra, and K. B. Mohanty, "Parameters estimation of photovoltaic module using nonlinear least square algorithm: A comparative study," in *Proc. Annu. IEEE India Conf.*, 2013, pp. 1–6.

[22] Y. A. Mahmoud, W. Xiao, and H. H. Zeineldin, "A parameterization approach for enhancing PV model accuracy," *IEEE Trans. Ind. Electron.*, vol. 60, no. 12, pp. 5708–5716, Dec. 2013.

[23] M. N. Islam, M. Z. Rahman, and S. M. Mominuzzaman, "The effect of irradiation on different parameters of monocrystalline photovoltaic solar cell," *Proc. 3rd Int. Conf. Develop. Renewable Energy Technol.*, 2014, pp. 1–6.

Emerson A. Silva was born in Jaboatao dos Guararapes, Brazil, in 1990. He received the B.Sc. degree in electrical engineering from the University of Pernambuco, Recife, Brazil, and the M.Sc. degree in electrical engineering from the Federal University of Pernambuco, Recife, in 2012 and 2015, respectively. He is currently working toward the Ph.D. degree in electrical engineering with the Federal University of Pernambuco.

His research interests include modeling and maximum power point tracking of photovoltaic systems.

Fabricio Bradaschia (S'10–M'13) was born in Sao Paulo, Brazil, in 1983. He received the B.Sc., M.Sc., and Ph.D. degrees in electrical engineering from the Federal University of Pernambuco, Recife, Brazil, in 2006, 2008, and 2012, respectively.

From August 2008 to August 2009, he was a Visiting Scholar with the University of Alcal, Madrid, Spain. Since October 2013, he has been an Associate Professor with the Department of Electrical Engineering, Federal University of Pernambuco. His research interests include applications of power electronics in renewable energy systems and power quality, including pulse width modulation, converter topologies, and grid synchronization methods.

Marcelo C. Cavalcanti was born in Recife, Brazil, in 1972. He received the B.Sc. degree in electrical engineering from the Federal University of Pernambuco, Recife, in 1997 and the M.Sc. and Ph.D. degrees in electrical engineering from the Federal University of Campina Grande, Campina Grande, Brazil, in 1999 and 2003, respectively.

From October 2001 to August 2002, he was a Visiting Scholar with the Center for Power Electronics Systems, Virginia Polytechnic Institute and State University, Blacksburg, VA, USA, and with University of Alcal, Madrid, Spain, from September 2012 to August 2013. Since 2003, he has been with the Department of Electrical Engineering, Federal University of Pernambuco, where he is currently a Professor of electrical engineering. His research interests include applications of power electronics in renewable energy systems and power quality.

Aguinaldo J. Nascimento, Jr. was born in Recife, Brazil, in 1986. He received the B.Sc. and M.Sc. degrees in physics from the Federal Rural University of Pernambuco, Recife, in 2010 and 2014, respectively. He is currently working toward the Ph.D. degree in electrical engineering with the Federal University of Pernambuco.

His research interests include modeling and maximum power point tracking of photovoltaic systems.